Supporting Information

Driver et al. 10.1073/pnas.0912130107

SI Text

We computed high-pressure high-temperature properties of silica by combining static QMC with DFT phonons from linear response in the quasiharmonic approximation for vibrational contributions. Here, additional analysis shows the behavior of bulk moduli, volume differences, thermal expansivity, heat capacity, and the Grüneisen ratio.

Bulk Moduli. Fig. S1 shows the calculated temperature and pressure dependencies of the bulk moduli of quartz, stishovite, and α-PbO_2. The bulk moduli decrease linearly with temperature and increase linearly with pressure for all pressure-temperature ranges. Although it is well known that DFT bulk moduli can vary significantly with choice of functional, results with the WC functional tend to lie only slightly below QMC. Both DFT and QMC agree with the experimental data for quartz (1) and stishovite (2) at zero pressure. No measurements are yet available for the elastic moduli of the α-PbO_2 phase.

Percent Volume Difference. Fig. S2 shows the computed QMC and WC volume differences for quartz-stishovite and $CaCl_2$-α-PbO_2 at 0 K. The quartz-stishovite volume change is large due to the four to six fold coordination change. The volume change in the $CaCl_2$-α-PbO_2 transition is roughly a factor of ten smaller.

Thermal Expansivity. Fig. S3 shows the computed QMC and WC thermal expansivity for quartz, stishovite, and α-PbO_2. In quartz, QMC and DFT both agree well with experimental measurements (2–8) at zero pressure. Experimentally, the quartz structure transforms to the β phase around 846 K, when the volume thermally expands to about 900 $Bohr^3$ and the thermal expansivity becomes negative. However, the computations presented here consider only the α-quartz phase. QMC and DFT also show good agreement with the measured stishovite expansivity. There have been no expansivity measurements for α-PbO_2.

Heat Capacity. Fig. S4 shows the computed QMC and WC heat capacities for quartz, stishovite, and α-PbO_2. In all cases, the WC results almost exactly match QMC. The quartz and stishovite results agree well with experiment (2, 5). There have been no heat capacity measurements for the α-PbO_2 phase.

Grüneisen Ratio. The Grüneisen ratio quantifies the relationship between thermal and elastic properties of a solid, $\gamma = V(\partial P/\partial U)_V = \alpha K_T V/C_V$, where α is the thermal expansivity, K_T is bulk modulus, V is volume, and C_V is the heat capacity at constant volume. Fig. S5 shows the computed QMC and WC Grüneisen ratios. The computations show reasonable agreement with quartz data (9) available at low pressures. In general, γ initially decreases with pressure and increases at high pressures. For quartz, we find γ decreases with temperature, but for stishovite and α-PbO_2, γ increases with temperature.

1. Levien L, Prewitt CT, Weidner DJ (1980) Structure and elastic properties of quartz at pressure. *Am Mineral* 65:920–930.
2. Nishihara Y, Nakayama K, Takahashi E, Iguchi T, Funakoshi K (2005) P-V-T equation of state of stishovite to the mantle transition zone conditions. *Phys Chem Mineral* 31:660–670.
3. Kihara K (1990) An X-ray study of the temperature dependence of the quartz structure. *Eur J Mineral* 2:63–77.
4. Carpenter MA et al. (1998) Calibration of excess thermodynamic properties and elastic constant variations associated with the alpha ↔ beta phase transition in quartz. *Am Mineral* 83:2–22.
5. Barron THK, Collins JF, Smith TW, White GK (1982) Thermal expansion, Grüneisen functions and static lattice properties of quartz. *J Phys C Solid State* 15:4311–4326.
6. Ito H, Kawada K, Akimoto S (1974) Thermal expansion of stishovite, *Phys Earth Planet In* 8:277–281.
7. Weaver JS, Takahashi T, Bassett WA (1973) Thermal expansion of stishovite (abstr.). *EOS T Am Geophys Un* 54:475.
8. Doroshev AM, Galkin VM, Kuznetsov GN (1987) Thermal expansion of stishovite at 98–420 K. *Geokhimiya* 10:1463–1467. (English translation: (1988) *Geochem. Int.* 25:92).
9. Boehler R (1982) Adiabats of quartz, coesite, olivine, and magnesium oxide to 50 kbar and 1000 K, and the adiabatic gradient in the Earth's mantle. *J Geophys Res* 87:5501–5506.

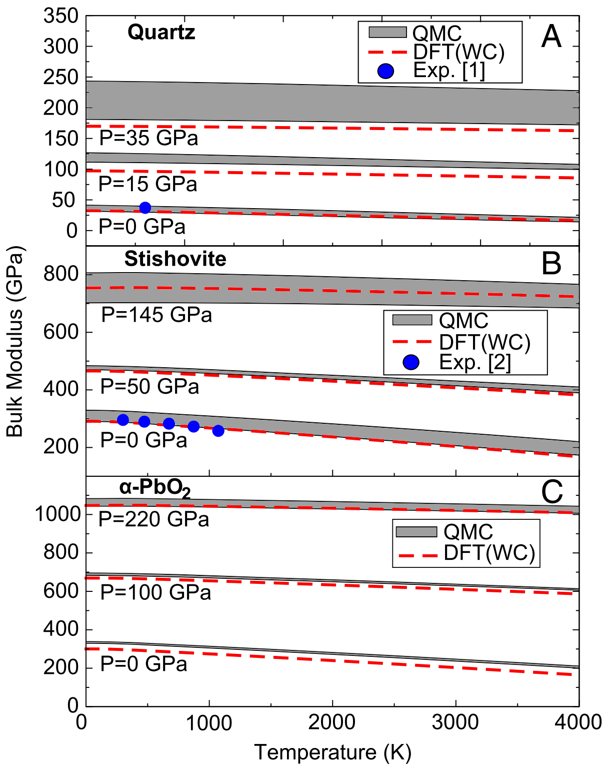

Fig. S1. Variation of the bulk modulus with temperature and pressure of (*A*) quartz, (*B*) stishovite, and (*C*) α-PbO_2. Gray shaded curves are QMC results, with the shading indicating one-sigma statistical errors. The dashed lines are DFT results using the WC functional. Solid circles are diamond anvil-cell data (1, 2) at 0 GPa.

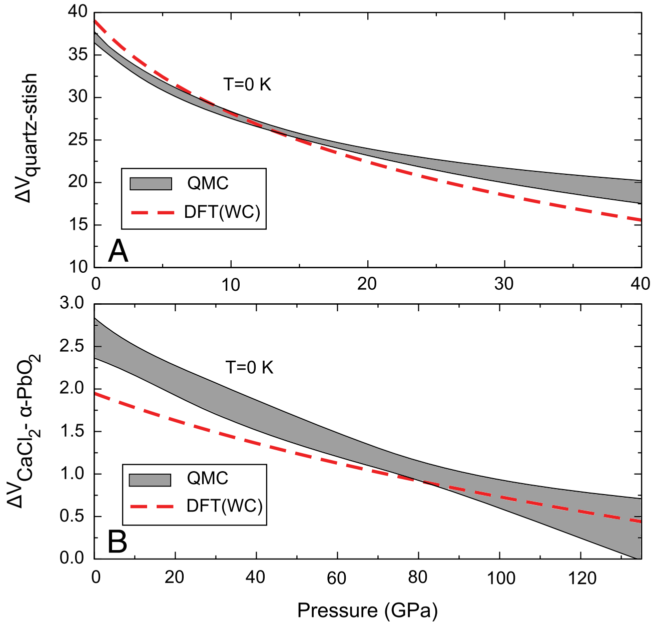

Fig. S2. Percentage volume difference of (*A*) quartz-stishovite and (*B*) $CaCl_2$-α-PbO_2 transitions. Gray shaded curves are QMC results, with the shading indicating one-sigma statistical errors. The dashed lines are DFT results using the WC functional.

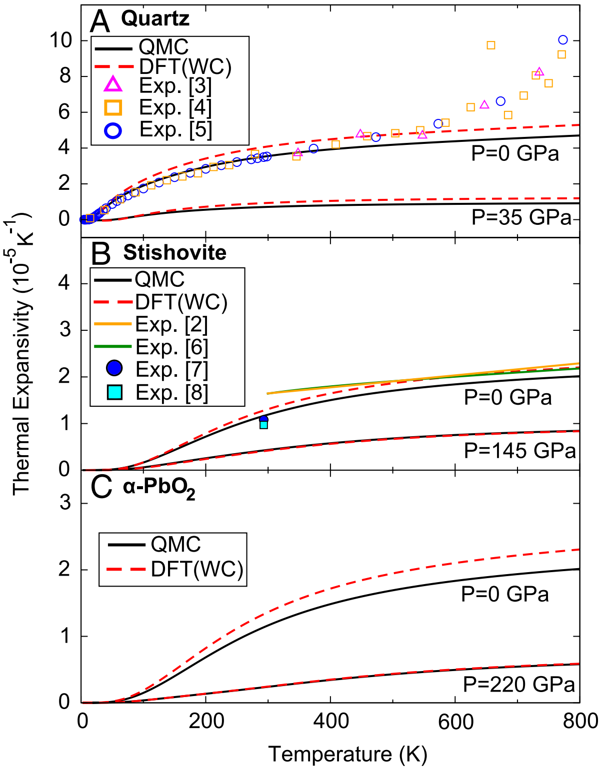

Fig. S3. Variation of the thermal expansivity with temperature and pressure of (*A*) quartz, (*B*) stishovite, and (*C*) α-PbO_2. Solid lines are QMC, where statistical errors are smaller than the line width, dashed lines are DFT using the WC functional, and the symbols are experimental measurements (2–8). Both QMC and DFT agree well with the experimental data for quartz and stishovite.

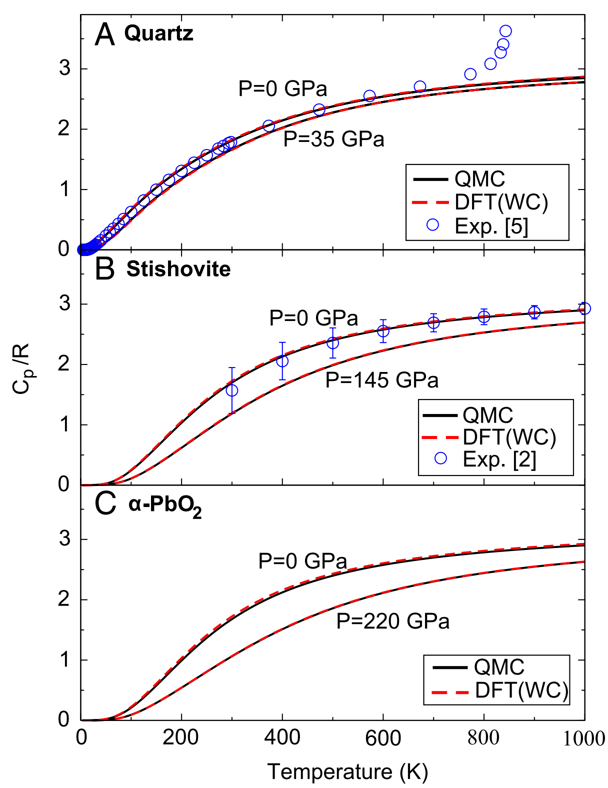

Fig. S4. Variation of the heat capacity with temperature and pressure of (*A*) quartz, (*B*) stishovite, and (*C*) α-PbO_2. Solid lines are QMC, where statistical errors are smaller than the line width, dashed lines are DFT using the WC functional, and symbols are experimental data (2, 5). Both QMC and DFT agree well with experimental data for quartz and stishovite.

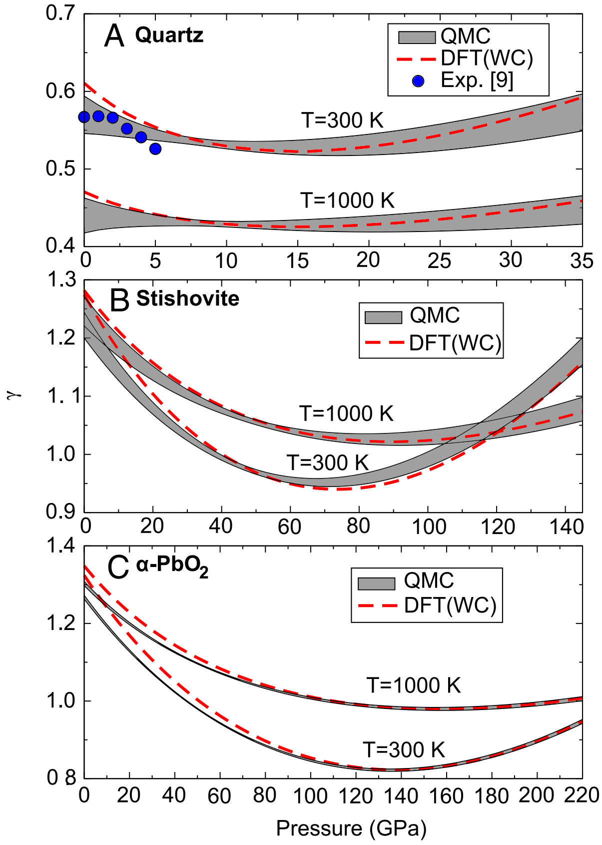

Fig. S5. Variation of the Grüneisen ratio with temperature and pressure of (*A*) quartz, (*B*) stishovite, and (*C*) α-PbO_2. Gray shaded curves are QMC results, with the shading indicating one-sigma statistical errors. The dashed lines are WC results. Solid circles are experimental data (9).